J Comp Physiol A (2013) 199:385–402
DOI 10.1007/s00359-013-0802-1

ORIGINAL PAPER

Ecomorphology of eye shape and retinal topography in waterfowl (Aves: Anseriformes: Anatidae) with different foraging modes

Thomas J. Lisney · Karyn Stecyk · Jeffrey Kolominsky · Brian K. Schmidt · Jeremy R. Corfield · Andrew N. Iwaniuk · Douglas R. Wylie

Received: 8 December 2012 / Revised: 12 February 2013 / Accepted: 13 February 2013 / Published online: 10 March 2013

Abstract Despite the large body of literature on ecomorphological adaptations to foraging in waterfowl, little attention has been paid to their sensory systems, especially vision. Here, we compare eye shape and retinal topography across 12 species representing 4 different foraging modes. Eye shape was significantly different among foraging modes, with diving and pursuit-diving species having relatively smaller corneal diameters compared to non-diving species. This may be associated with differences in ambient light intensity while foraging or an ability to tightly constrict the pupil in divers in order to facilitate underwater vision. Retinal topography was similar across all species, consisting of an oblique visual streak, a central area of peak cell density, and no discernible fovea. Because the bill faces downwards when the head is held in the normal posture in waterfowl, the visual streak will be held horizontally, allowing the horizon to be sampled with higher visual acuity. Estimates of spatial resolving power were similar among species with only the Canada goose having a higher spatial resolution. Overall, we found no evidence of ecomorphological adaptations to different foraging modes in the retinal ganglion cell layer in waterfowl. Rather, retinal topography in these birds seems to reflect the 'openness' of their habitats.

Keywords Duck · Feeding behavior · Retinal ganglion cell · Visual acuity · Visual streak

Abbreviations

A	Axial length
asf	Area-sampling fraction
C	Mean corneal diameter
CE	Coefficient of error
NA	Numerical aperture
PND	Posterior nodal distance
PrV	Principal sensory nucleus of the trigeminal nerve
RGC	Retinal ganglion cell
SRP	Spatial resolving power
T	Mean transverse eye diameter

T. J. Lisney (✉) · K. Stecyk · D. R. Wylie
Department of Psychology, University of Alberta, Edmonton, AB, Canada
e-mail: tomlisney@gmail.com

J. Kolominsky · D. R. Wylie
Centre for Neuroscience, University of Alberta, Edmonton, AB, Canada

B. K. Schmidt
Division of Birds, National Museum of Natural History, Smithsonian Institution, PO Box 30712, Washington, DC 20013-7012, USA

J. R. Corfield · A. N. Iwaniuk
Department of Neuroscience, Canadian Centre for Behavioural Neuroscience, University of Lethbridge, Lethbridge, AB, Canada

Introduction

The task of locating, acquiring, and utilizing food is vital for survival in all animals and is of central importance in ecology (Begon et al. 2006). Among birds, ducks, geese, and swans (Anseriformes: Anatidae) have proved especially useful for studying ecomorphological adaptations to different foraging modes and diet (Goodman and Fisher 1962; Rylander and Bolen 1974; Kehoe and Thomas 1987; Bock 1994; Nudds et al. 1994; Guillemain et al. 2002a; Gurd 2007). Although these birds typically spend a large amount of time sitting on the water and share a number of

common morphological adaptations to an aquatic lifestyle, they exhibit considerable variation in foraging behavior and diet (Johnsgard 1978; Bellrose 1980; del Hoyo et al. 1992; van der Leeuw et al. 2003). According to del Hoyo et al. (1992), the most common foraging modes are (1) grazing on terrestrial vegetation (as seen in many geese, tribe Anserini), (2) surface-feeding by dabbling or tipping up (dabbling ducks, tribe Anatini), and (3) diving. Among diving species, foraging tactics and diet vary from those of the diving ducks or pochards (tribe Aythyini), which make relatively shallow dives to feed on both aquatic vegetation and invertebrates, to those of the pursuit-diving mergansers (tribe Mergini), which dive to deeper depths to catch invertebrates and fishes.

Animals rely on their sensory systems to detect and guide them to food sources and these sensory systems show adaptations to the demands of a species' particular feeding behavior (Hayes and Brooke 1990; Martin and Katzir 1999; Rice and Westneat 2005; Temple et al. 2010). Tactile cues play a particularly important role in foraging in waterfowl (Gutiérrez-Ibáñez et al. 2009) and these birds possess many mechanoreceptors on their bills and tongues (Krogis 1931; Gottschaldt and Lausmann 1974; Leitner and Roumy 1974; Berkhoudt 1980). The overall number of mechanoreceptors and the relative proportions of pressure (Herbst's corpuscles) and velocity (Grandry's corpuscles) receptors vary among species in association with feeding behavior (Krogis 1931; Kear and Burton 1971; Gottschaldt and Lausmann 1974; Berkhoudt 1980). Interspecific variation in the importance of tactile sensory information in foraging in waterfowl is further reflected by variation in the relative size of the initial processing area in the brain for tactile sensory information, the principal sensory nucleus of the trigeminal nerve (PrV) (Gutiérrez-Ibáñez et al. 2009).

In contrast to the somatosensory system, little is known about variation in the visual system among waterfowl. For example, the organization of the eye and retina is only known for the mallard, *Anas platyrhynchos* (Martin 1986; Jane and Bowmaker 1988; Braekevelt 1990; Rahman et al. 2007a) and the Canada goose, *Branta canadensis* (Fernández-Juricic et al. 2011; Moore et al. 2012). Nevertheless, behavioral studies indicate that vision plays a more important role in some species than in others (Tome and Wrubleski 1988). Furthermore, ducks that rely more on visual cues when foraging have more frontally positioned eyes than tactile feeders (Goodman and Fisher 1962; Guillemain et al. 2002b; Martin et al. 2007). Visual feeders also tend to have a larger binocular visual field overlap than tactile feeders and the bill occupies a more central position within the frontal binocular field, thus allowing for more accurate visual control of bill position (Martin 1986; Guillemain et al. 2002b; Martin et al. 2007). In addition, the accommodative mechanism differs between diving and non-diving ducks. Underwater, the refractive power of the cornea is lost and to compensate this, diving ducks such as the hooded merganser (*Lophodytes cucullatus*) and the common goldeneye (*Bucephala clangula*) that rely on vision to find prey underwater are able to change the shape of their lenses to greatly increase the optical power of the eye (Levy and Sivak 1980; Sivak et al. 1985). In comparison, accommodation in non-diving, dabbling ducks such as the mallard and the wood duck (*Aix sponsa*) is an order of magnitude less (Sivak et al. 1985).

The aforementioned evidence notwithstanding, the paucity of comparative data on the visual system in waterfowl means it is difficult to evaluate to what extent the organization of the eyes of these birds are correlated with different foraging modes. We therefore conducted a detailed study of eye shape and retinal topography in 12 species, representing 4 different foraging modes: (1) grazing, (2) dabbling, (3) diving, and (4) pursuit-diving. Both eye shape and retinal topography are particularly useful in understanding the ecomorphology of the visual system in birds (e.g. Wathey and Pettigrew 1989; Hayes and Brooke 1990; Inzunza et al. 1991; Boire et al. 2001; Coimbra et al. 2006, 2009, 2012; Hall and Ross 2007; Dolan and Fernández-Juricic 2010; Iwaniuk et al. 2010a; Corfield et al. 2011; Fernández-Juricic et al. 2011; Lisney et al. 2012a, b). We investigated eye shape because it is a predictor of activity pattern in vertebrates; species active in dim light generally have a larger cornea, relative to eye size, than species active under brighter conditions (Hughes 1977; Pettigrew et al. 1988; Kirk 2004, 2006; Hall and Ross 2007; Schmitz and Wainwright 2011; Lisney et al. 2012a, b). A number of species of waterfowl are active and feed at night, while others, such as the pursuit-diving mergansers, appear to be limited to foraging under brighter conditions (del Hoyo et al. 1992; McNeil et al. 1992; Lewis et al. 2005). Therefore, we predicted that interspecific variation in eye shape would reflect variation in foraging behavior. Second, the topographic organization of retinal cells and the location of specialized areas of high cell density for acute vision in the retinal ganglion cell (RGC) layer are closely matched to feeding behavior in vertebrates (Collin 1999, 2008), including birds (Budnik et al. 1984; Moroney and Pettigrew 1987; Hayes and Brooke 1990; Inzunza et al. 1991; Rahman et al. 2007a; Dolan and Fernández-Juricic 2010). Thus, our second prediction was that the topographic distribution, total number, and/or density of cells in the RGC layer would vary among waterfowl species and be associated with different foraging modes. For example, we predicted that tactile and/or nocturnal feeders such as dabbling ducks would exhibit lower total cell numbers and cell densities than diving species that rely more heavily on vision. In addition, we predicted that pursuit-diving species reliant on vision would have

retinal specializations situated in the temporal retina, which would allow the frontal visual field, including the region of binocular overlap, to be viewed with a higher spatial resolving power, thus facilitating the detection of food items the control of accurate bill position.

Materials and methods

Study species

Eyes from 12 species of waterfowl representing 4 tribes (Anserini, Anatini, Aythyini, and Mergini) were used in this study: Canada goose (*Branta canadensis*), northern shoveler (*Anas clypeata*), blue-winged teal (*Anas discors*), mallard (*Anas platyrhynchus*), gadwall (*Anas strepera*), American wigeon (*Anas americana*), redhead (*Aythya americana*), canvasback (*Aythya valisineria*), lesser scaup (*Aythya affinis*), greater scaup (*Aythya marila*), hooded merganser (*Lophodytes cucullatus*), and red-breasted merganser (*Mergus serrator*) (Table 1). The eyes were collected from hunters in Alberta, Canada, or from specimens in the Division of Birds collection at the National Museum of Natural History (Washington, DC, USA; see "Appendix"). In all cases, the entire head was immersion fixed in 4 % paraformaldehyde or 10 % formalin. For the museum specimens, we only processed material that had been kept in 10 % formalin and not transferred to 70 % ethanol, as is common practice in museum collections. The specimens were left in fixative for at several weeks prior to extracting the eyes.

Each species was categorized as having one of four different foraging modes based on reports in the literature: (1) grazing, (2) dabbling, (3) diving, and (4) pursuit-diving (Table 1).

Eye morphology

Before being removed from the head, the limbus of each eye was marked with colored nail varnish dorsally and naso-ventrally in line with angle of the bill. This ensured that we could subsequently orientate the eyes and retinas into their natural position after excision. After excision, the transverse diameters of the eyeball and the cornea were measured along two perpendicular planes using digital calipers, as described in Lisney et al. (2012b). In total, measurements were made from 32 eyes from 20 individual birds. At least two eyes per species were used, with the exceptions of the Canada goose and the blue-winged teal, for which only one eye was available for study. We then calculated the ratio of mean corneal diameter (C) to mean transverse eye diameter (T), the C:T ratio (Kirk 2004, 2006), as a measure of eye shape. In a number of previous studies of eye morphology in vertebrates, the diameters of the eye and cornea have been measured from eyes that were 'reinflated' with fixative using a syringe and a small-gauge needle (e.g. Kirk 2004, 2006; Hall and Ross 2007; Lisney et al. 2012a, b). In this study, we found that the majority of the eyes (66 %) could not be reinflated because of small cuts in the sclera that either occurred during the dissection process or were purposely made in order to facilitate the infusion of fixative into the vitreous chamber. However, in the transverse plane, the uninflated eyes still closely resembled the shape of the eyes that could be reinflated. Using the eyes that could be reinflated, we confirmed that there was no significant difference between C:T ratios calculated from corneal and eye diameter measurements made before and after reinflation (paired t test on $\log_{10}$ transformed data, $t = 1.802$, $df = 10$, $p = 0.1018$). Moreover, following Lessells and Boag (1987), we calculated that our measurements had a high degree of repeatability ($r = 0.884$). Recently, we have also shown that in another avian order, the Galliformes, there is no significant difference in the C:T ratios calculated using measurements made on eyes before and after reinflation (Lisney et al. 2012b). Therefore, we are confident in our use of measurements made from uninflated eyes to calculate C:T ratios.

For the eyes that could be reinflated, the axial length (A) of the eye was also measured (Hall and Ross 2007; Iwaniuk et al. 2010a; Lisney et al. 2012a, b). As well as being used in the calculation of peak theoretical anatomical spatial resolving power (see below) eye axial length was used to calculate another measure of eye shape, the C:A ratio (Kirk 2006; Hall and Ross 2007; Veilleux and Lewis 2011; Lisney et al. 2012a, b). Both the C:T and C:A ratios provide a measure of cornea size relative to the total size of the eye (Kirk 2006) and higher values for both ratios are consistently found in animals that live in dim light compared to animals that live in higher light levels (Pettigrew et al. 1988; Kirk 2004, 2006; Hall and Ross 2007; Schmitz and Wainwright 2011; Veilleux and Lewis 2011; Lisney et al. 2012a, b).

Retinal whole mounts

After measuring eye and corneal diameter, small cuts (piercing the sclera and the retina) were made through the nail varnish marks to denote dorsal and bill angle orientation. The eyes were then hemisected and the retinas were dissected out. From the 32 eyes, 28 retinas were successfully whole mounted. For each retina, the retinal pigment epithelium was bleached using a solution of 20 % hydrogen peroxide in phosphate buffered saline at room temperature for 24 h (Lisney et al. 2012a, b). After bleaching, the vitreous was removed, the pecten was cut off at the

Table 1 Information on the taxonomy, foraging mode, and diet of the 12 species of waterfowl used in this study

Tribe	Species	Common name	Foraging mode	Diet
Anserini (Swans and geese)	*Branta canadensis*	Canada goose	Grazing	Grasses roots, stems, leaves, fruits and green parts of aquatic plants and sedges; also grain and cereal crops
Anatini (Dabbling ducks)	*Anas americana*	American wigeon	Dabbling	Grasses, sedges, herbs and greener parts of crop and aquatic plants
	Anas clypeata	Northern shoveler	Dabbling	Small-sized aquatic invertebrates (insects and their larvae, molluscs, crustaceans); also small floating plants, seeds and plant remains
	Anas discors	Blue-winged teal	Dabbling	Seeds and vegetative parts of aquatic plants but will also take aquatic invertebrates
	Anas platyrhynchos	Mallard	Dabbling	Omnivorous and opportunistic, feeding on seeds and vegetative parts of aquatic and crop plants, terrestrial and aquatic invertebrates, amphibians and fish
	Anas strepera	Gadwall	Dabbling	Aquatic vegetation; occasionally grazes grasses and cereals by walking on land
Aythyini (Diving ducks)	*Aythya affinis*	Lesser scaup	Diving	Aquatic invertebrates such as insect larvae, crustaceans, and molluscs. Seeds and other plant material also eaten
	Aythya americana	Redhead	Diving	Seeds, leaves and stems of grasses, sedges, algae and other aquatic plants, tubers, grain. Will also take aquatic invertebrates
	Aythya marila	Greater scaup	Diving	Prefers molluscs, especially clams. Other food types include invertebrates and small fish, roots, seeds and vegetative parts of aquatic plants and sedges
	Aythya valisineria	Canvasback	Diving	Feeds on a variety of aquatic vegetative and animal matter
Mergini (Sea ducks)	*Lophodytes cucullatus*	Hooded merganser	Pursuit-diving	Fish and aquatic invertebrates; also takes amphibians and some plant material
	Mergus serrator	Red-breasted merganser	Pursuit-diving	Small freshwater or marine fish; also aquatic invertebrates and some plant material

Information presented in the table taken from Johnsgard (1978), Bellrose (1980) and del Hoyo et al. (1992)

base or removed entirely, and each retina was whole mounted RGC layer uppermost, and stained for Nissl substance using 0.1 % Cresyl Violet (pH 4.3), as described previously (Stone 1981; Ullmann et al. 2012; Lisney et al. 2012a, b). In order to assess shrinkage of the retinal whole mounts, the outline of each whole mount pre- and post-staining was traced from scaled digital photographs using the public domain NIH image program ImageJ (Rasband 1997–2012) (Lisney et al. 2012a, b). Average shrinkage was 3.5 ± 2.1 % and was confined to the margins of the whole mount and along the edges of the radial relieving cuts or tears (Stone 1981).

Cell counts

The distribution of Nissl-stained cells in the RGC layer of each whole mount was assessed using systematic random sampling and the fractionator principle (Gundersen 1977; Coimbra et al. 2009, 2012; Lisney et al. 2012a, b). Using a sampling grid measuring 1 × 1 mm, digital photo-micrographs of the RGC layer were taken at regular intervals across each whole mount using one of two microscope imaging systems: (1) a Leica DMRE compound microscope with a ×100 oil immersion objective (numerical aperture, NA = 1.3) equipped with a Retiga EXi *FAST* Cooled mono 12-bit camera (Qimaging, Burnaby, BC, Canada) and Openlab imaging software (Improvision, Lexington, MA, USA), and (2) a Leitz Labourlux S compound microscope with a ×100 oil immersion objective (NA = 1.25), equipped with a IMC-4050FT camera (Imi Tech, Encinitas, CA, USA), a MS-2000 XYZ automated stage and control unit (Applied Scientific Instrumentation, Eugene, OR, USA) and Stereologer software (Stereology Resource Center, http://www.disector.com).

An unbiased counting frame (35 × 35 μm) was imposed in the centre of each digital photomicrograph using ImageJ. We counted cells if they lay entirely within the counting frame or if they touched an acceptance line without touching a rejection line (Gundersen 1977). Glial cells, which were identified based on their small size, elongate 'spindle'- or 'cigar'-like shape and dark staining (Hughes 1985; Wathey and Pettigrew 1989; Coimbra et al. 2009) were not included in the counts. We did not differentiate between RGCs and 'displaced' amacrine cells (Ehrlich 1981; Hayes 1984; Chen and Naito 1999; Hart 2002) in any of the whole mounts because we could not reliably distinguish between the two cell types using cytological criteria, especially in the areas of high cell density.

Topography maps and total cell numbers

The cell counts for each counting frame were converted to cell densities (cells mm^{-2}). Our retinal topography maps are interpolated isodensity contour plots created using DeltaGraph 6 (Red Rock Software, Salt Lake City, UT, USA) (Ahnelt et al. 2006; Schiviz et al. 2008; Lisney et al. 2012b). The scaled, correctly oriented post-stain outline of each whole mount, traced from a digital photograph (see above), was then superimposed on top of the contour plot to complete the topography map. To determine the total number of cells in the RGC layer for each whole mount, we multiplied the total number of cells counted by the inverse of the area-sampling fraction (asf), which is the area of the counting frame divided by the area of the sampling grid. For example, for a 35 × 35 μm counting frame and a 1 × 1 mm sampling grid, the asf = 0.001225 mm^2. Coefficients of error (CE) were calculated using Schaeffer's estimator for a one-stage systematic sample (Scheaffer et al. 1996) for non-homogeneous distributions (Schmitz and Hof 2000). As a CE of ≤0.10 is considered highly reliable (Boire et al. 2001; Coimbra et al. 2009, 2012; Ullmann et al. 2012) our CEs, which were all ≤0.044 (Table 2), show that our estimates of total number of cells in the whole mounts are robust.

Spatial resolving power

We estimated the visual acuity of seven of the species by calculating their theoretical peak anatomical spatial resolving power (SRP; expressed in cycles/deg), following Hart (2002). Because a measure of the focal length of the eye is required to calculate SRP using this method, we were restricted to the species for which we were able to measure eye axial length (see Table 2). The posterior nodal distance (PND; the distance from the lens centre to the choroid–retina border) was used as a measure of focal length (Hart 2002; Lisney and Collin 2008; Lisney et al. 2012b; Ullmann et al. 2012) and was assumed to be ×0.6 of the eye axial length (Hughes 1977; Martin 1994a; Ullmann et al. 2012).

Statistical analysis

Statistical analyses were performed using Prism 5 (GraphPad Software, San Diego, CA, USA). All data were $\log_{10}$ transformed prior to analysis. Because of the relatively small numbers of species in each of the four foraging mode categories, we were only able to perform statistical tests (unpaired *t* tests) comparing C:T ratio and total number of cells and average and peak cell densities in the RGC layer between the two most speciose of these categories, dabbling and diving. Correlations between C:A and

Table 2 Summary of eye shape data for the 12 species of waterfowl used in this study

Species	*Branta canadensis*	*Anas americana*	*Anas clypeata*	*Anas discors*	*Anas platyrhynchos*	*Anas strepera*	*Aythya affinis*	*Aythya americana*	*Aythya marila*	*Aythya valisineria*	*Lophodytes cucullatus*	*Mergus serrator*
Common name	Canada goose	American wigeon	Northern shoveler	Blue-winged teal	Mallard	Gadwall	Lesser scaup	Redhead	Greater scaup	Canvasback	Hooded merganser	Red-breasted merganser
Foraging mode	Grazing	Dabbling	Dabbling	Dabbling	Dabbling	Dabbling	Diving	Diving	Diving	Diving	Pursuit-diving	Pursuit-diving
Eye shape												
Average eye transverse diameter (T) (mm)	23.14	15.02	13.44 ± 0.54	12.93	15.86 ± 0.41	14.01 ± 0.59	13.80	15.23	15.20 ± 0.58	15.36 ± 0.40	15.68	15.19 ± 0.06
	(*n* = 1)	(*n* = 2)	(*n* = 4)	(*n* = 1)	(*n* = 3)	(*n* = 5)	(*n* = 2)	(*n* = 2)	(*n* = 4)	(*n* = 3)	(*n* = 2)	(*n* = 3)
Average corneal diameter (C) (mm)	14.13	7.78	8.00 ± 0.45	7.45	8.61 ± 0.18	8.02 ± 0.62	6.65	7.81	7.28 ± 0.09	7.65 ± 0.34	7.90	7.13 ± 0.44
	(*n* = 1)	(*n* = 2)	(*n* = 4)	(*n* = 1)	(*n* = 3)	(*n* = 5)	(*n* = 2)	(*n* = 2)	(*n* = 4)	(*n* = 3)	(*n* = 2)	(*n* = 3)
Eye shape (C:T)	0.61	0.52	0.60 ± 0.06	0.58	0.54 ± 0.003	0.57 ± 0.04	0.48	0.51	0.48 ± 0.01	0.50 ± 0.02	0.50	0.47 ± 0.03
	(*n* = 1)	(*n* = 2)	(*n* = 4)	(*n* = 1)	(*n* = 3)	(*n* = 5)	(*n* = 2)	(*n* = 2)	(*n* = 4)	(*n* = 3)	(*n* = 2)	(*n* = 3)
Eye axial diameter (A) (mm)	20.97	–	12.00	–	13.30	12.40	12.50	–	13.30	–	–	12.50
	(*n* = 1)		(*n* = 1)		(*n* = 2)	(*n* = 2)	(*n* = 2)		(*n* = 2)			(*n* = 1)
Eye shape (C:A)	0.67	–	0.67	–	0.65	0.65	0.53	–	0.55	–	–	0.57
	(*n* = 1)		(*n* = 1)		(*n* = 2)	(*n* = 2)	(*n* = 2)		(*n* = 2)			(*n* = 1)

Average values are presented, along with ±1 standard deviation (SD) for the species for which data for three or more eyes were available. The number of eyes assessed for each species (*n*) is given in parentheses

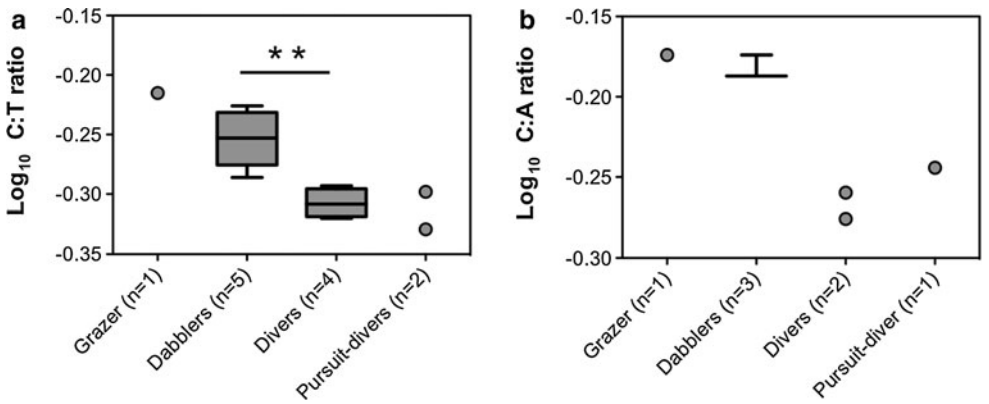

Fig. 1 Box-and-whisker/dot plots showing eye shape in waterfowl with different foraging modes. Eye shape is expressed using $\log_{10}$ transforms of **a** the ratio of mean corneal diameter to mean transverse eye diameter (C:T) and **b** the ratio of mean corneal diameter to axial eye diameter (C:A). The asterisks in **a** indicate that there was a significant difference ($p = 0.0043$) in C:T ratio between dabbling and diving ducks

C:T ratios and total cell number and whole mount area were tested using Pearson product–moment correlation coefficients.

Results

Eye shape

C:T ratios ranged from 0.61 in the Canada goose to 0.47 in the red-breasted merganser (Table 2). Non-diving waterfowl that feed by grazing or dabbling had higher C:T ratios than diving and pursuit-diving species (Fig. 1a). There was a significant difference in C:T ratio between dabbling and diving ducks ($t = 4.148$, $p = 0.0043$). A similar trend was seen in the C:A ratios (Table 2; Fig. 1b) but because of the smaller sample sizes, differences in C:A ratio between dabbling and diving species were not tested statistically. Average C:A ratios were significantly correlated with average C:T ratios (Pearson's $r = 0.926$, $p = 0.003$).

Retinal topography

The density of cells in the RGC layer varied across the retina in a similar fashion in all 12 species (Figs. 2, 3, 4). The lowest cell densities, in the order of 2,000–3,000 cells mm^{-2}, were found in the dorsal and ventral peripheries. More centrally, a visual streak running across the retina was evident, containing cell densities $\geq$10,000 cells mm^{-2}. The visual streak was not oriented horizontally parallel to the angle of the bill, but rather ran at an oblique angle (approximately 20–25 deg) from nasal-dorsal to temporal-ventral (Fig. 3). In all species, the peak cell densities (ca. 17,000–25,000 cells mm^{-2}) (Fig. 5a) were found within the visual streak in the central retina close to the superior pole of the pecten. We did not observe a foveal pit associated with the area of peak cell density in any of our whole mounts. The cells in the peripheral retina and in the visual streak were relatively heterogeneous in terms of size, compared to the more homogenous population of small cells found in the central retina around the area of peak cell density (Fig. 2). The similarities in retinal topography among species with different feeding modes are revealed by comparing the isodensity contour retinal topography maps (Fig. 3), and the density profiles along dorso-ventral transects across the retina, passing through the area of peak cell density (Fig. 4).

Total cells, cell densities, and SRP

In the majority of the 12 species, the total number of cells in the RGC layer ranged from approximately 1.4 to 1.7 million (Table 3). Total cell number was much higher in the Canada goose (3,055,510) and, to a lesser extent, the mallard (2,150,204). However, the whole mounts for these two species had the greatest area (424 and 250 mm^2, on average, respectively), compared to the other waterfowl (154–230 mm^2; Table 3). The total number of cells in the RGC layer was significantly correlated with whole mount area (Pearson's $r = 0.940$, $p < 0.0001$). The total number of cells was similar among dabbling, diving, and pursuit-diving species (Fig. 5b) and there was no significant difference in the total cell number between dabbling and diving species ($t = 0.367$, $p = 0.725$). Average cell density ranged from 7,068 cells mm^{-2} in the canvasback to 8,986 cells mm^{-2} in the redhead (Table 3). Average cell densities were similar among foraging modes (Fig. 5c) and there was no significant difference between average cell density in dabbling and diving species ($t = 1.835$, $p = 0.109$). As mentioned above, peak cell densities ranged from approximately 17,000–25,000 cells mm^{-2} with the lowest value found in the blue-winged teal and the highest value found in the lesser scaup (Table 3). Peak cell

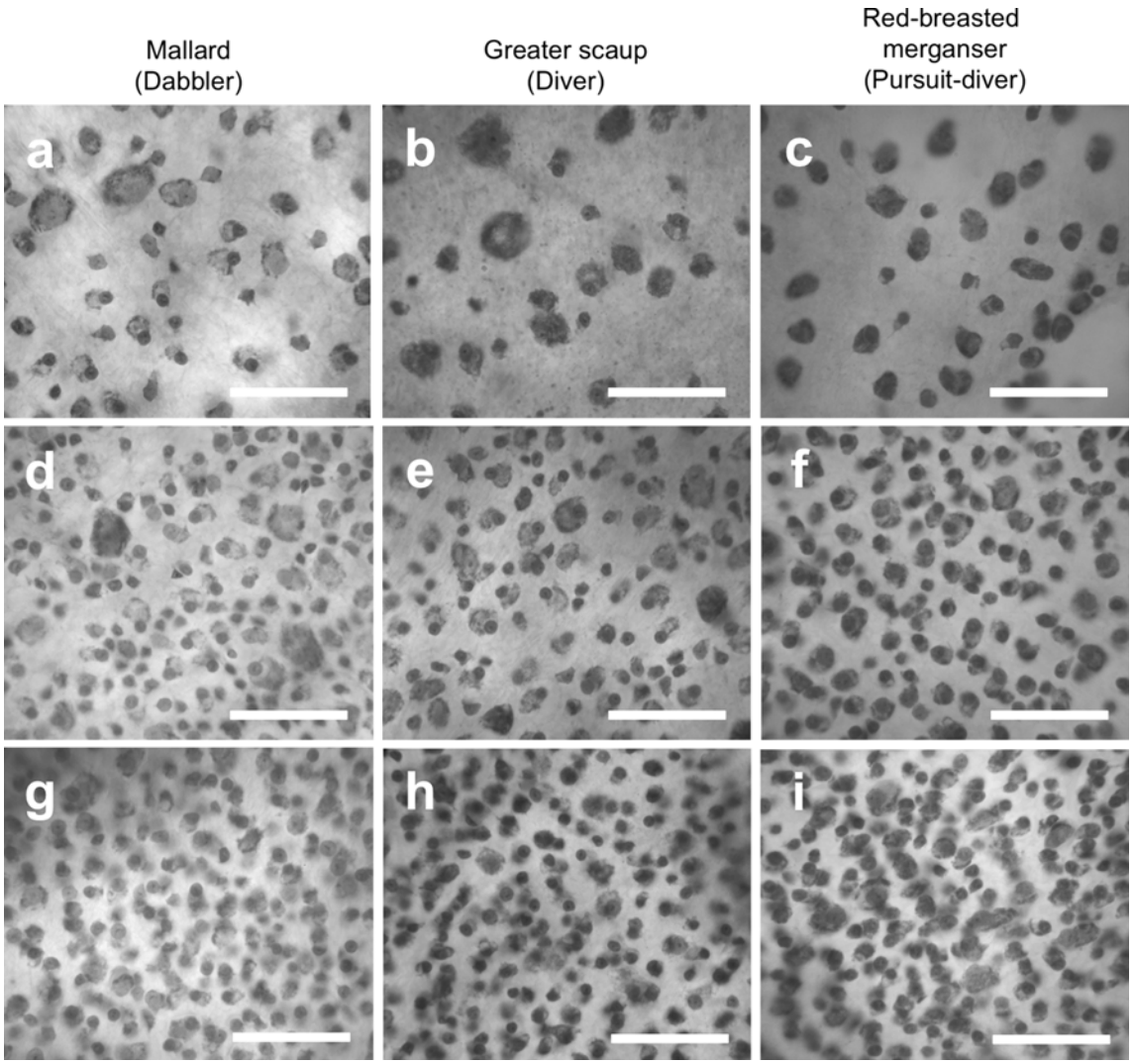

Fig. 2 High magnification digital photo-micrographs showing Nissl-stained cells in the retinal ganglion cell layer in three species of waterfowl with different foraging modes; the mallard (**a**, **d**, **g**), greater scaup (**b**, **e**, **h**) and red-breasted merganser (**c**, **f**, **i**). **a–c** Cells at low densities in the dorsal periphery, **d–f** Cells at intermediate densities in the visual streak, **g–i** cells at high densities in the central retina in the area of peak cell density. *Scale bars* represent 40 μm

densities were similar among foraging modes (Fig. 5a) and there was no significant difference between dabbling and diving species ($t = 0.216$, $p = 0.836$).

Theoretical peak anatomical SRP was calculated for seven species (Table 3; Fig. 5d). SRP was similar in six of the seven species, representing dabbling, diving, and pursuit-diving, ranging from an average of 10.1 cycles/deg in the gadwall to 11.9 cycles/deg in the mallard. In contrast, SRP for the Canada goose was much higher at 16.9 cycles/deg.

Discussion

The various morphological adaptations to different foraging modes in waterfowl serve as a classic example of ecomorphology (Goodman and Fisher 1962; Bock 1994; Guillemain et al. 2002a). However, to date there have been few attempts to evaluate whether the organization of the sensory systems also vary in relation to foraging mode in these birds. To this end, we assessed variation in two important visual system traits, eye shape and retinal topography, in 12 species of waterfowl. Representatives of four different foraging modes: grazing, dabbling, diving, and pursuit diving, were included in our study. Overall, we found evidence for differences in eye shape among foraging modes, but retinal topography was similar among all of the species we investigated, irrespective of their foraging mode.

Eye shape

A number of studies have shown that eye shape is closely and consistently associated with the environmental

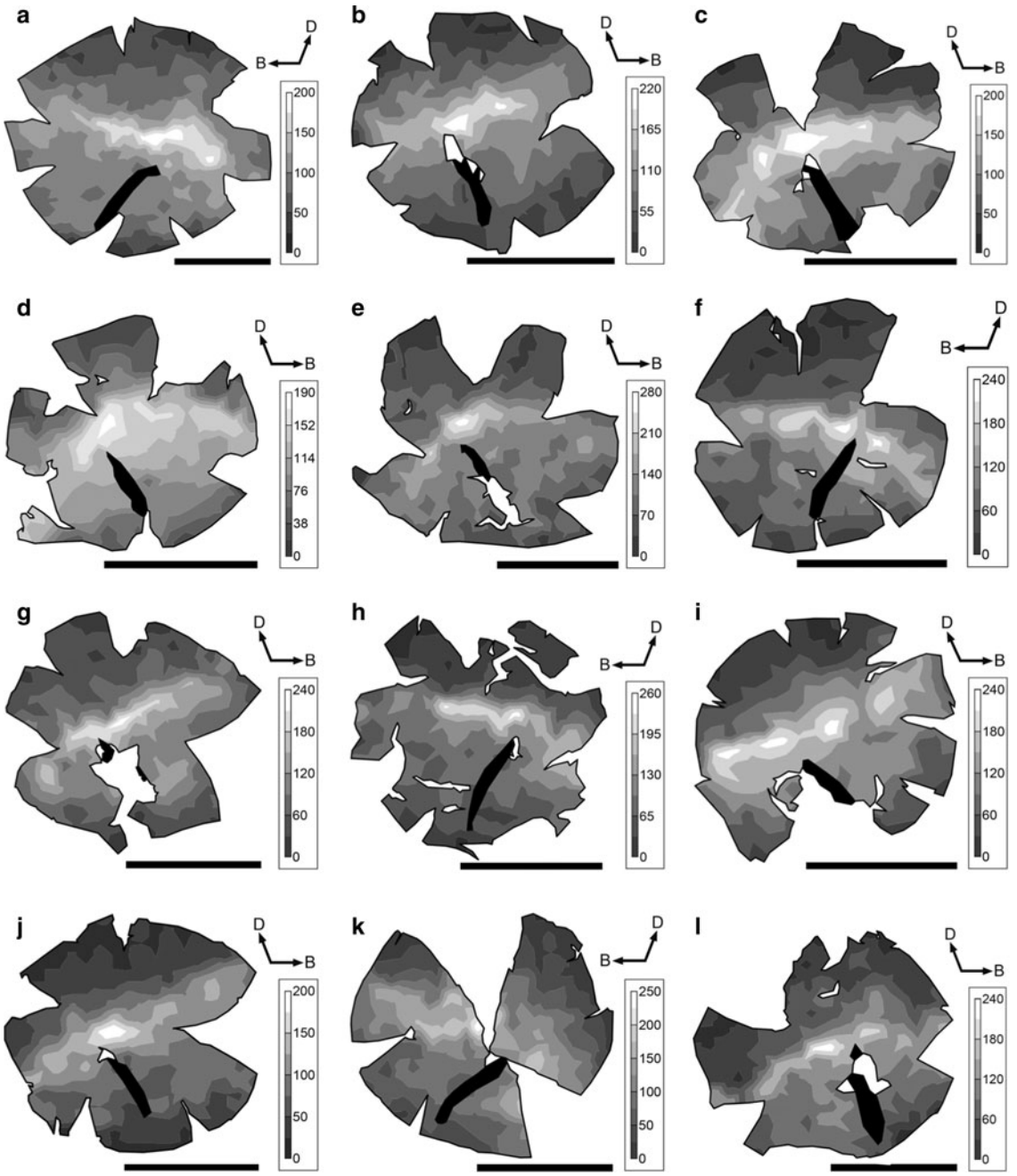

Fig. 3 Representative isodensity contour maps illustrating the topographic distribution of cells in the retinal ganglion cell layer in 12 species of waterfowl with different foraging modes. **a** Left retina from the Canada goose (grazer). **b** Right retina from the American wigeon (dabbler). **c** Right retina from the northern shoveler (dabbler). **d** Right retina from the blue-winged teal (dabbler). **e** Right retina from the mallard (dabbler). **f** Left retina from the gadwall (dabbler). **g** Right retina from the lesser scaup (diver). **h** Left retina from the redhead (diver). **i** Right retina from the greater scaup (diver). **j** Right retina from the canvasback (diver). **k** Left retina from the hooded merganser (pursuit-diver). **l** Right retina from the red-breasted merganser (pursuit-diver). The orientation *arrows* for each map indicate the angle of the bill (B) and dorsal (D). Note that the maps have been positioned so that the bill angle is horizontal. The shaded density scales, which are different among species, represent $\times 10^3$ cells mm^{-2}. The irregular black shapes on each map represent the position of the pecten. *Scale bars* represent 10 mm

light conditions under which a species is most active (e.g. Kirk 2004, 2006; Hall and Ross 2007; Schmitz and Wainwright 2011; Veilleux and Lewis 2011; Lisney et al. 2012a, b). A relatively larger cornea acts to enhance visual sensitivity because the size of the cornea constrains the total amount of light that can enter the eye when the pupil is maximally dilated (Kirk 2006). Therefore, species that are active under dim light

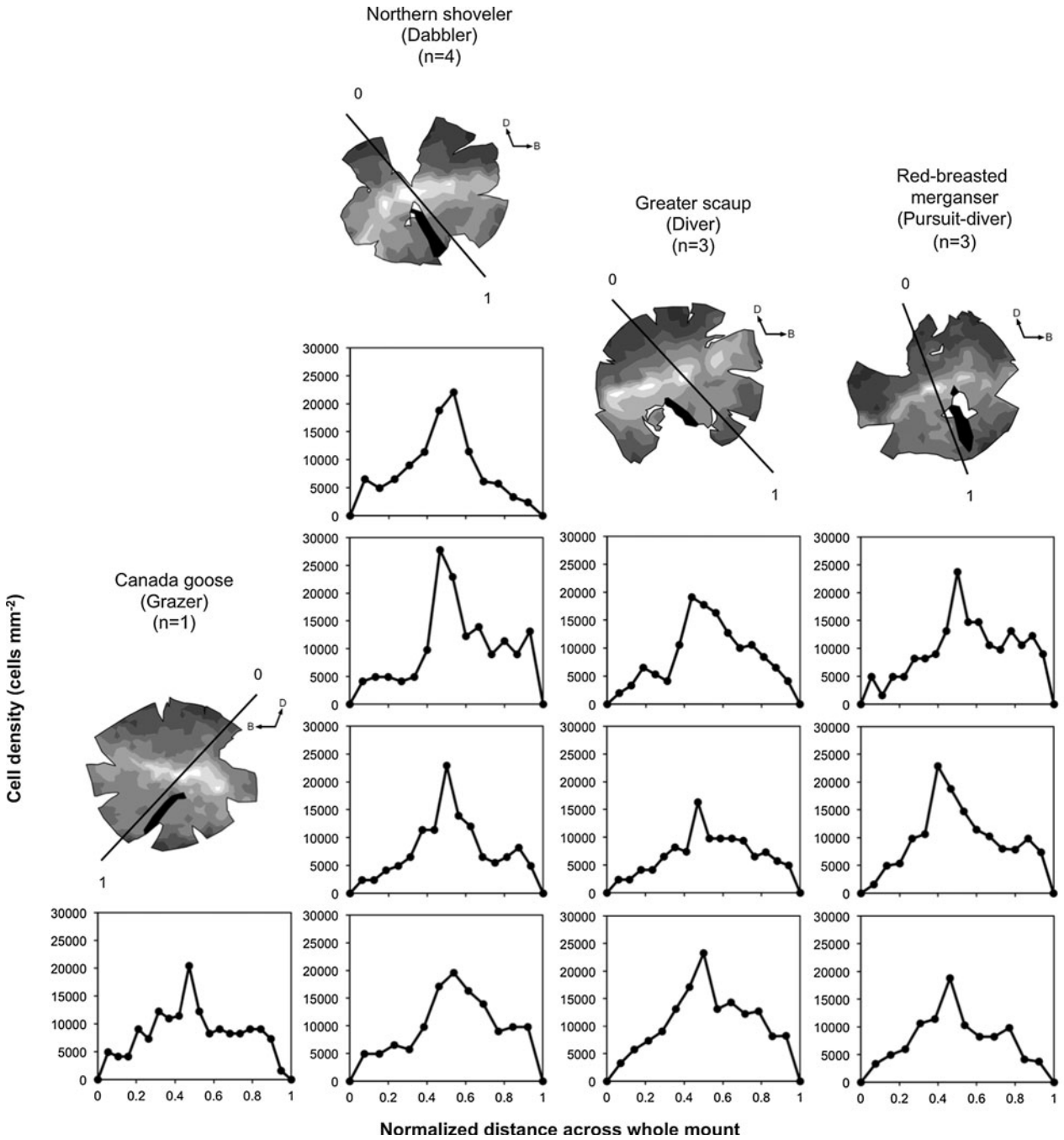

Fig. 4 Density profiles for cells in the retinal ganglion cell layer measured along dorso-ventral transects (0–1) across the retina in four species of waterfowl with different foraging modes. The transects run from the dorsal (0) to the ventral (1) edge of each whole mount, and pass through the central area of peak cell density, as indicated on the isodensity contour maps for each species. Orientation *arrows* have been included for each map, indicating the angle of the bill (B) and dorsal (D) (as in Fig. 3). The distance across each retina was been standardized on a scale of 0–1 allowing direct comparisons of the density profiles. For three species, the northern shoveler, greater scaup, and red-breasted merganser, the density profiles for multiple retinas are presented. Note the similarities in the density profiles both within and among species

conditions tend to have relatively larger corneas than species active under brighter conditions.

In waterfowl, we found C:T ratios ranging from 0.47 to 0.61. Our value of 0.61 for the Canada goose is the same as the C:T ratio calculated from values provided in Fernández-Juricic et al. (2011). Overall, the C:T ratios for waterfowl are lower than those found in strictly nocturnal owls (0.67–0.69), but the C:T ratios in the two pursuit-diving species and some of the diving ducks are similar to those found in diurnal birds (0.45–0.50), such as the pigeon

Table 3 Summary of retinal topography data for the 12 species of waterfowl used in this study

Species	*Branta canadensis*	*Anas americana*	*Anas clypeata*	*Anas discors*	*Anas platyrhynchos*	*Anas strepera*	*Aythya affinis*	*Aythya americana*	*Aythya marila*	*Aythya valisineria*	*Lophodytes cucullatus*	*Mergus serrator*
Common name	Canada goose	American wigeon	Northern shoveler	Blue-winged teal	Mallard	Gadwall	Lesser scaup	Redhead	Greater scaup	Canvasback	Hooded merganser	Red-breasted merganser
Foraging mode	Grazing	Dabbling	Dabbling	Dabbling	Dabbling	Dabbling	Diving	Diving	Diving	Diving	Pursuit-diving	Pursuit-diving
Retinal topography												
Peak cell density (cells mm^{-2})	20,400 ($n = 1$)	21,225 ($n = 2$)	24,896 ± 3,918 ($n = 4$)	17,143 ($n = 1$)	23,401 ± 3,681 ($n = 3$)	21,633 ± 1,414 ($n = 4$)	25,306 ($n = 2$)	24,898 ($n = 2$)	21,111 ± 4,147 ($n = 3$)	18,503 ± 1,699 ($n = 3$)	22,041 ($n = 2$)	21,769 ± 2,624 ($n = 3$)
Total number of cells	3,055,510 ($n = 1$)	1,556,441 ($n = 2$)	1,465,714 ± 109,112 ($n = 4$)	1,353,469 ($n = 1$)	2,150,204 ± 71,109 ($n = 3$)	1,565,510 ± 186,877 ($n = 4$)	1,388,980 ($n = 2$)	1,698,776 ($n = 2$)	1,463,401 ± 155,025 ($n = 3$)	1,622,858 ($n = 2$)	1,510,923 ($n = 2$)	1,653,878 ($n = 2$)
CE	0.016 ($n = 1$)	0.025 ($n = 2$)	0.042 ± 0.006 ($n = 4$)	0.036 ($n = 1$)	0.028 ± 0.007 ($n = 3$)	0.044 ± 0.014 ($n = 3$)	0.041 ($n = 2$)	0.040 ($n = 2$)	0.038 ± 0.003 ($n = 3$)	0.023 ($n = 2$)	0.029 ($n = 2$)	0.032 ($n = 2$)
Whole mount area (mm^2)	424 ($n = 1$)	204 ($n = 2$)	168 ± 4.7 ($n = 4$)	154 ($n = 1$)	250 ± 8.5 ($n = 3$)	183 ± 13.8 ($n = 4$)	192 ($n = 2$)	190 ($n = 2$)	201 ± 6.3 ($n = 3$)	230 ($n = 2$)	184 ($n = 2$)	219 ($n = 2$)
Average cell density (cells mm^{-2})	7,206 ($n = 1$)	7,637 ($n = 2$)	8,734 ± 614 ($n = 4$)	8,763 ($n = 1$)	8,606 ± 382 ($n = 3$)	8,527 ± 421 ($n = 4$)	7,253 ($n = 2$)	8,986 ($n = 2$)	7,304 ± 887 ($n = 3$)	7,086 ($n = 2$)	8,189 ($n = 2$)	7,487 ($n = 2$)
PND (mm) (Eye axial diameter × 0.6)	12.58 ($n = 1$)	–	7.2 ($n = 1$)	–	7.98 ($n = 2$)	7.44 ($n = 2$)	7.5 ($n = 2$)	–	7.98 ($n = 2$)	–	–	7.5 ($n = 1$)
SRP (cycles/deg)	16.9 ($n = 1$)	–	11.2 ($n = 1$)	–	11.9 ($n = 2$)	10.1 ($n = 2$)	11.2 ($n = 2$)	–	11.2 ($n = 1$)	–	–	10.8 ($n = 1$)

Average values are presented along with ±1 standard deviation (SD) for the species for which data for three or more eyes were available. The number of retinas assessed for each species (n) is given in parentheses

CE coefficients of error for the estimates of the total numbers of cells in the retinal ganglion cell layer, *PND* posterior nodal distance, *SRP* spatial resolving power

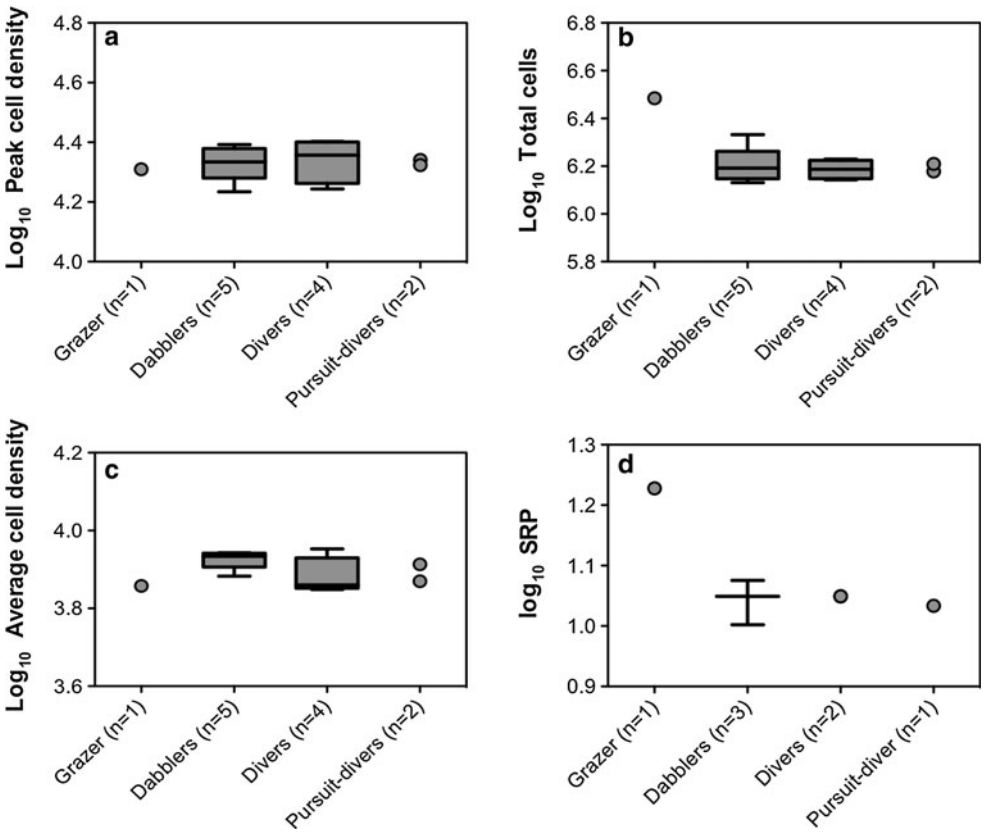

Fig. 5 Box-and-whisker/dot plots showing variation in the peak (**a**) and average (**c**) densities and total numbers (**b**) of cells in the retinal ganglion cell layer and peak theoretical anatomical spatial resolving power (SRP) (**d**) among waterfowl with different foraging modes. All data have been $\log_{10}$ transformed

(*Columba livia*), hummingbirds, and hawks (Lisney, unpublished data). The Canada goose, a grazing species, and dabbling ducks have higher C:T ratios than the diving and pursuit-diving ducks. The relatively low ratios in the latter are consistent with observations that these ducks are visual feeders and that their foraging is restricted to times of relatively high light intensities (Sjöberg 1985, 1988; Lewis et al. 2005). Similarly, the relatively high ratios in the dabbling ducks are congruous with the crepuscular and nocturnal foraging patterns of these birds (McNeil et al. 1992; Guillemain et al. 2002c). In contrast, despite having the highest C:T ratio of any of the species we investigated, the Canada goose does not appear to exhibit any preference for nocturnal feeding, but rather may feed at anytime (Raveling et al. 1972; Jorde and Owen 1988; McNeil et al. 1992). Moreover, like dabbling ducks, diving ducks in general show preferences for crepuscular and/or nocturnal feeding (del Hoyo et al. 1992; McNeil et al. 1992; Custer et al. 1996), yet here we found C:T ratios in diving ducks to be significantly lower than in dabbling ducks. A reason for this apparent discrepancy may be that it is not actually possible to simply define temporal variation in foraging in these birds as being diurnal, crepuscular, or nocturnal. The timing of foraging activities in most waterfowl appears to be highly adaptable, varying in relation to a range of factors including geographical location, season, weather conditions, lunar and tidal cycle, food availability, and predation risk (Jorde and Owen 1988). Specific information on activity pattern is lacking for most waterfowl and thus it has proved difficult to correlate activity pattern with specific foraging modes (Jorde and Owen 1988).

Alternatively, because the ability to constrict the pupil down to a small diameter can facilitate amphibious vision (Gislén et al. 2003) and because corneal diameter is closely related to pupil size (Kirk 2004, 2006; Hall and Ross 2007), it may be advantageous for diving and pursuit-diving ducks to have relatively smaller corneal diameters compared to non-diving species. The refractive power of the cornea is lost underwater, resulting in a severely blurred image in eyes lacking a high power spherical lens (as found in fish eyes, for example) to compensate for this lack of refractive power (Land and Nilsson 2002). This can be offset by constricting the pupil to produce a sharper image with greater depth of field, thus significantly improving visual acuity (Gislén et al. 2003; Land and Nilsson 2002). Furthermore, diving and pursuit-diving ducks are able to change the shape of the lens by tightly constricting the pupil (down to a diameter of 1 mm; Levy and Sivak 1980) and pushing the malleable lens against the rigid iris disc such that the central part of the lens bulges through the pupil. This serves to greatly increase the optical power of the eye and thus improve visual performance underwater (Levy and Sivak 1980; Sivak et al. 1985).

'Displaced' amacrine cells

The RGC layer contains both the RGCs and 'displaced' amacrine cells. Of the two, the RGCs are the axon-bearing output neurons of the retina and represent the only link between the eye and the brain (Hughes 1977; Pettigrew et al. 1988). In birds, estimates of the proportion of cells in the RGC layer accounted for by the displaced amacrine cells range from almost zero in the Japanese quail *Coturnix japonica* (Budnik et al. 1984; Ikushima et al. 1986), 11 % in the pigeon (Hayes 1984), 20–35 % in the chicken *Gallus gallus* (Ehrlich and Morgan 1980; Ehrlich 1981; Chen and Naito 1999) and 50 % in the barn owl (Wathey and Pettigrew 1989). Little information exists for waterfowl, but Ma et al. (2004) reported that, on average 33 % of the cells in the RGC layer are amacrine cells in a domesticated breed of the mallard, the Beijing duck.

In this study, we counted of all the Nissl-stained cells in the RGC layer, which means that the displaced amacrine cell population has been included in our data. We did this because, although cytological criteria have been proposed to differentiate between RGCs and amacrine cells in avian Nissl-stained whole mounts (Ehrlich 1981; Hayes 1984; Chen and Naito 1999; Hart 2002), it can be very difficult to distinguish between these two cell types in the central retina and other areas of high cell density (Hughes 1977; Stone 1981; Wathey and Pettigrew 1989; Coimbra et al. 2006, 2009; Pang and Wu 2011; Lisney et al. 2012a, b). We do not consider that the inclusion of the displaced amacrine cells in our cell counts has significantly affected our findings for two reasons. First, in species for which RGC topography has been assessed using both Nissl staining and retrograde labeling, the peak cells densities and the overall retinal topography remain similar despite the inclusion of the displaced amacrine cells (Pettigrew et al. 1988; Collin 1999). Second, because cells counts from the RGC layer are converted to cell density (cells mm^{-2}) and then reduced to the square root in order to calculate SRP, large differences in peak cell densities result in only a small difference in terms of SRP (Pettigrew et al. 1988; Ullmann et al. 2012). For example, if we assume that 33 % of the cells in the area of peak cell density in the mallard are displaced amacrine cells (Ma et al. 2004), our revised peak cell density becomes 15,679 cells mm^{-2}, but our estimate of peak SRP for this species only drops from 11.9 to 9.4 cycles/deg.

Retinal topography

The retinal topography in all 12 species was characterized by an oblique visual streak (relative to the angle of the bill) and a central area of peak cell density. A similar pattern of retinal topography was described in the mallard and the Canada goose (Rahman et al. 2007a; Fernández-Juricic et al. 2011; Moore et al. 2012), while Wood's (1917) macroscopic and ophthalmological studies revealed an oblique visual streak in a number of additional waterfowl species.

Visual streaks are characteristically associated with animals that live in open habitats dominated by an unobstructed horizon. They allow an animal to sample a broad horizon with increased visual acuity, without the need for extensive eye or head movements (Hughes 1977; Collin 1999, 2008). Irrespective of their particular foraging mode, waterfowl typically spend much of their time sitting on the water, meaning that the horizon (be it the interface of the sky and/or the land with the waters' surface) predominates their visual fields. The Canada goose also lives in open habitats, such as grasslands and cultivated fields when it is grazing on terrestrial vegetation (del Hoyo et al. 1992; Fernández-Juricic et al. 2011). Therefore, rather than showing ecomorphological adaptations to particular foraging modes, retinal topography in waterfowl seems to reflect the symmetry or 'openness' of their habitats, in accordance with Hughes' (1977) 'terrain' theory.

To optimize visual sampling of the horizon, a visual streak should be oriented parallel to said horizon (Hughes 1977). Why then does the visual streak in waterfowl appear to be orientated at an oblique angle? Like some other birds, waterfowl display 'klinorhynchy'. That is, when the head is held in the normal posture, the bill faces downwards (Duijm 1958; Martin 1986, 1994b; Land 1999; Guillemain et al. 2002b; Martin et al. 2007; Martin and Shaw 2010). In waterfowl, this downward angle is commonly ca. 20–30 deg (Martin 1986; Guillemain et al. 2002b; Martin et al. 2007; Fernández-Juricic et al. 2011; Fig. 6). As we found that the visual streak runs at an oblique angle of approximately 20–25 deg relative to the angle of the bill in these birds, this strongly indicates that when the head is in the normal posture, the visual streak will actually be held horizontally (Duijm 1958; Land 1999). Canada geese reportedly hold their heads such that the bill is held horizontal, yet during scanning behavior, this species does orient its head so the bill is pointing downwards (Fernández-Juricic et al. 2011). Because the visual streak is also aligned with the lateral semicircular canal in birds, it may also serve to quickly and accurately establish the normal position of the eye, which would be important for spatial orientation (Duijm 1958; Collin 1999). In contrast, when the head is raised or lowered during feeding, flight or behavioral displays (Johnsgard 1965; Raveling 1969; Fernández-Juricic et al. 2011), the angle of the visual streak will become oblique. This orientation would allow different parts of the visual field to be sampled with a higher SRP and, in certain head positions, the ground and the sky to be viewed simultaneously (Fernández-Juricic et al. 2011; Moore et al. 2012).

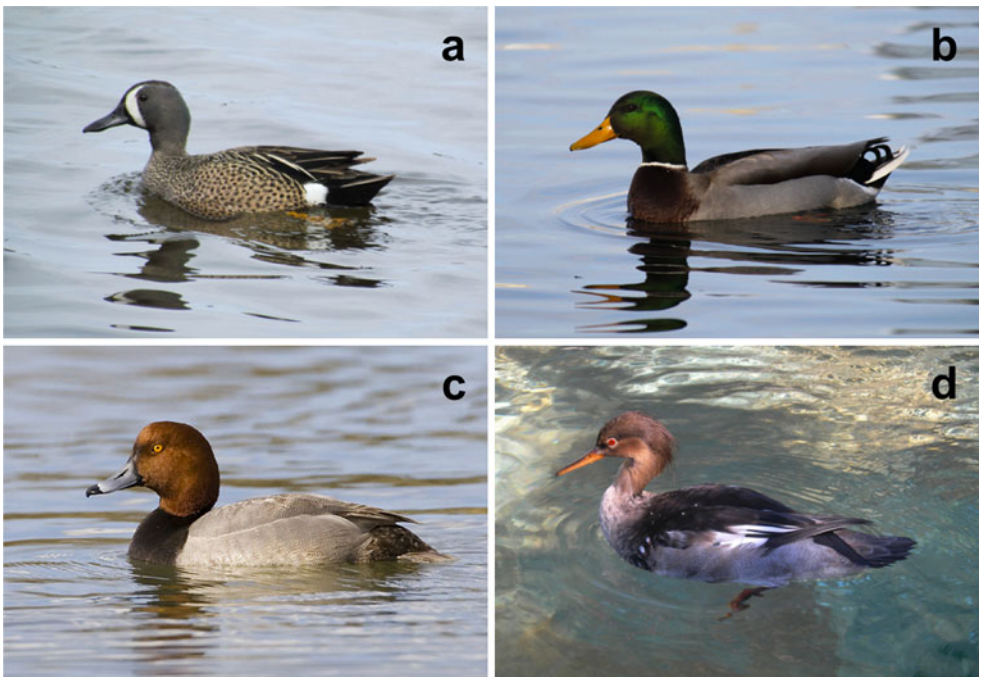

Fig. 6 Representative photographs showing four species of waterfowl with their heads the normal posture. Note that the bill is facing downwards at an angle of ca. 20–30 deg. **a** Blue-winged teal. **b** Mallard. **c** Redhead, courtesy of and reproduced with permission of Gerald Romanchuk, Canada. **d** Red-breasted merganser

Waterfowl face threats from a variety of aerial and terrestrial predators (del Hoyo et al. 1992; Sargeant and Raveling 1992). The presence of a visual streak, in combination with eyes which are, to a greater or lesser extent laterally placed (resulting in large monocular visual fields) (Martin 1986; Guillemain et al. 2002b; Martin et al. 2007; Fernández-Juricic et al. 2011) indicates that vision is particularly important for predator surveillance in these birds. Furthermore, the visual streak may also play an important role during flight. Waterfowl undertake daily flights from roost sites to feeding areas and most species are migratory (Johnsgard 1978; Bellrose 1980; del Hoyo et al. 1992). When airborne, the visual streak could help birds orient themselves with respect to both the horizon and conspecifics when flying in formation (Land 1999; Fernández-Juricic et al. 2011).

All 12 species of waterfowl possessed a small area of peak cell density in the central retina. A centrally positioned area of peak cell density (though not necessarily associated with a visual streak), which may or may not include a fovea, is perhaps the most common retinal specialization seen in birds (Meyer 1977; Dolan and Fernández-Juricic 2010). These peak density areas are presumably involved in monocular vision and would allow an area of the lateral or frontal-lateral visual field on either side of the head to be viewed with a higher SRP (Hayes et al. 1987), depending on the position of the eyes in the head and the degree of eye movement among species (Goodman and Fisher 1962; Martin 1986; Guillemain et al. 2002b; Martin et al. 2007; Fernández-Juricic et al. 2011). In contrast to the large monocular visual fields found in waterfowl, the binocular visual field tends to be relatively narrow (ca. 20–30 deg) and extends from just below the bill to behind the head (Martin 1986; Guillemain et al. 2002b; Martin et al. 2007; Fernández-Juricic et al. 2011). In retinal whole mounts, it is not possible to determine which part of the visual field is subtended by a specific retinal area (Ullmann et al. 2012), but presumably the binocular visual field in waterfowl is subtended by parts of the peripheral temporal and ventral retina. Thus, other than the temporal-most part of the visual streak, does not appear to be associated with any retinal specializations for visual acuity.

Total cells, cell densities, and SRP

The total number, and peak and average densities of cells in the RGC layer, as well as estimates of theoretical peak anatomical SRP, were similar among dabbling, diving and pursuit-diving ducks. Although the Canada goose has a much higher total number of cells than any of the other species we investigated, this is a consequence of it having a much larger eye and retina. Indeed, the average cell density in the Canada goose is similar to that of the other 11 species (Table 2). The Canada goose's large eye also means that this species has a greater PND and so a higher SRP compared to the other species (Fernández-Juricic et al.

Table 4 Comparison of retinal topography data in waterfowl with other birds

	Peak cell density in RGC layer (cells mm^{-2})	Total cells in RGC layer/total putative RGCs ($\times 10^6$)	Average cell density (cells mm^{-2})	SRP (cycles/deg)	References
Ostrich (*Struthio camelus*)	9,500	2.27	900	22.6	Boire et al. (2001)
Penguins (Spheniscidae)	10,000 to 21,867	1.11–1.72	865–2,200	12.8–15.3[a]	Suburo et al. (1991), Coimbra et al. (2012)
Barn owl (*Tyto alba*)	12,500 to 19,100	1.22–1.40	4,200–6,100	10	Wathey and Pettigrew (1989), Lisney et al. (2012a)
Seabirds (Procellariiformes)	8,900 to 21,500	0.60–3.01	1,600–6,300	–	Hayes and Brooke (1990)
Waterfowl (Anatidae)	11,300 to 24,000	1.35–3.05	3,000–8,600	10.1–16.9	This study; Rahman et al. (2007a), Fernández-Juricic et al. (2011)
Gamefowl (Phasianidae)	22,100 to 35,600	1.51–3.31	8,300–15,400	9.7–20.6	Ehrlich (1981), Ikushima et al. (1986), Hart (2002), Lisney et al. (2012b)
Strigid owls (Strigidae)	23,000 to 34,000	1.95–6.92	7,400–13,900	12–15[b]	Fite (1973), Lisney et al. (2012a)
Songbirds (Passeriformes)	21,700 to 26,200	1.60–3.59	6,100–18,500	4.7–7.6	Rahman et al. (2006, 2007b, 2008), Dolan and Fernández-Juricic (2010)
Pigeon (*Columba livia*)	40,000 to 41,000	2.38	–	14.7[c]	Binggeli and Paule (1969), Marshall et al. (1973), Hayes and Holden (1983)
Diurnal hawks and eagles (Falconiformes)	38,000 to 68,000	–	–	73–143[b]	Reymond (1985, 1987), Inzunza et al. (1991)
Tyrant flycatchers (Tyrannidae)	48,000 to >150,000	1.92–4.15	26,100–32,900	–	Coimbra et al. (2006, 2009)
Kingfishers (Coraciiformes)	140,000 to 180,000	–	–	26–41	Moroney and Pettigrew (1987)

To make comparisons among different birds easier, the values for peak cell density, total cells and average cell density have been rounded up to the nearest 100, 10,000 and 100, respectively

[a] Values refer to SRP in air; to estimate SRP underwater multiply value by 1.333 (Coimbra et al. 2012)

[b] SRP determined behaviorally

[c] Calculated following Hart (2002), using a peak cell density of 41,000 cells mm^{-2} (Hayes and Holden 1983) and a PND of 7.72 mm (Marshall et al. 1973)

2011; Lisney et al. 2012b). The potential for greater visual acuity in this species may permit better visual control of beak position and facilitate the identification of small food items on the ground or discriminating between more or less nutritious parts of plants (Fernández-Juricic et al. 2011).

For some waterfowl, we found a fairly high degree of inter-individual variation in the total cell and cell density values, reflected by large standard deviations (Table 3). A similar degree of inter-individual variation has been previously reported in fishes (Collin and Ali 1994; Collin et al. 1998; Lisney and Collin 2008), birds (Dolan and Fernández-Juricic 2010; Fernández-Juricic et al. 2011) and mammals (Mass and Supin 1995; Mass et al. 2011). This suggests that such individual variation in the organization of the RGC layer may be common in vertebrates. The functional consequences of this variation on visual performance among individuals may not be great because, for example, large differences in peak cell densities only result in small differences in SRP (Pettigrew et al. 1988; Ullmann et al. 2012).

In Table 4, the total number of cells in the RGC layer, peak and average cell densities and SRP in waterfowl are compared with the values for other birds. Collectively, the values for waterfowl are most similar to those in the barn owl (*Tyto alba*), gamebirds, and seabirds. This means that waterfowl have relatively low numbers of cells in the RGC layer compared to a number of avian groups, such as pigeons, diurnal raptors, tyrant flycatchers, and kingfishers. These birds are considered heavily reliant on vision and possess at least one well-developed fovea, a specialization for acute vision (Slonaker 1897; Walls 1942; Fite and Rosenfield-Wessels 1975; Meyer 1977; Moroney and Pettigrew 1987; Inzunza et al. 1991; Coimbra et al. 2006, 2009). In contrast, we did not detect a fovea associated

with the area of peak cell density in any of our waterfowl whole mounts. Heppner et al. (1965) and Rahman et al. (2007a) did not identify a fovea in the Canada goose and the mallard, respectively (although Fernández-Juricic et al. (2011) observed a putative fovea in the former), while Slonaker (1897) and Wood (1917) reported various waterfowl species as either lacking a fovea or having a small or poorly developed fovea. Overall then, it would appear that waterfowl are either afoveate, or that they possess relatively shallow foveas compared to those found some other groups of birds and therefore the waterfowl retina is relatively unspecialized for high visual acuity. This, along with the relatively low numbers of their cells in the RGC, is consistent with Iwaniuk et al.'s (2010b) recent finding that tectofugal brain regions in waterfowl are significantly smaller relative to brain volume compared other birds. Overall, we consider that waterfowl rely less on acute vision for feeding than other birds and rather place a greater emphasis on tactile sensory information (Gutiérrez-Ibáñez et al. 2009; Iwaniuk et al. 2010b).

Conclusions and future directions

In conclusion, we found evidence for differences in eye shape among waterfowl with different foraging mode that may reflect differences in light availability at the times when these birds are foraging. However, given that the timing of foraging activities in waterfowl can be highly variable both among and within species, and the information on nocturnal activity is lacking for most species, it is currently difficult to evaluate relationships between eye shape and foraging activity until such information becomes available. Moreover, the relatively smaller corneal diameters found in diving and pursuit-diving ducks could be associated with an ability to tightly constrict the pupil in order to facilitate underwater vision in these birds. In contrast to the variation in eye shape, our results reveal that the overall topography of cells in the RGC layer is relatively uniform in waterfowl, despite differences in feeding mode.

A detailed analysis of the specific topographic distribution of different size-classes of presumed RGCs has revealed retinal specializations related to foraging in birds (Hayes et al. 1991; Suburo et al. 1991; Coimbra et al. 2006, 2009, 2012) and a similar analysis on waterfowl retinas may yet identify similar specializations not detected in our study. Alternatively, even if the organization of the RGC layer is similar across waterfowl (reflecting the generally 'open' nature of the environments inhabited by these birds), ecomorphological adaptations to different foraging modes may be present in other aspects of visual system organization. For example, there is some interspecific variation in eye movements and visual field among waterfowl (Martin 1986; Guillemain et al. 2002b; Martin et al. 2007; Fernández-Juricic et al. 2011), but representatives of some foraging modes, such as diving (Aythyini) and pursuit-diving (Mergini) have not been studied at all. Another direction worthy of future research concerns the assessment of the relative proportions of different cone types across the retina, which is related to ecological factors, including foraging mode in birds (Partridge 1989; Hart 2001). Finally, where possible future studies should include species with foraging modes that were not available to us in this study, such as diving species like eider ducks and scooters (Merginae) that feed on hard-bodied invertebrates, or species that rely heavily on vision and clear waters for feeding, such as the New Zealand blue duck *Hymenolaimus malacorhynchos* (Martin et al. 2007).

Acknowledgments All of our methods adhered to Canadian Council for Animal Care Guidelines and were approved by the University of Lethbridge Animal Welfare Committee. We wish to thank George Iwaniuk, Greg Sanbourn, Udo Hannebaum and the curatorial staff of the Division of Birds for providing specimens for this study. Gerald Romanchuk kindly allowed us to use his photograph of a redhead. Heather Lisney and Vincent and Angela Galipeau provided essential support during the preparation of the paper. Funding was provided by the Natural Sciences and Engineering Council of Canada (NSERC) Discovery Grants and Discovery Accelerator Supplements to ANI and DRW.

Appendix

See Table 5.

Table 5 List of specimens from the Division of Birds collection at the National Museum of Natural History (Washington, DC, USA) used in this study

Species	Common name	Specimen number(s)
Aythya marila	Greater scaup	USNM643756
		USNM643757
Aythya valisineria	Canvasback	USNM643732
		USNM643733
Lophodytes cucullatus	Hooded merganser	USNM643735
Mergus serrator	Red-breasted merganser	USNM643761

References

Ahnelt PK, Schubert C, Kübber-Heiss A, Schiviz A, Anger E (2006) Independent variation of retinal S and M cone photoreceptor topographies: a survey of four families of mammals. Vis Neurosci 23:429–435

Begon M, Townsend CR, Harper JL (2006) Ecology: from individuals to ecosystems, 4th edn. Blackwell, Oxford

Bellrose FC (1980) Ducks, geese and swans of North America, 3rd edn. Stackpole Books, Harrisburg

Berkhoudt H (1980) The morphology and distribution of cutaneous mechanoreceptors (Herbst and Grandry corpuscles) in bill and tongue of the mallard (*Anas platyrhynchos L.*). Neth J Zool 50:1–34

Binggeli RL, Paule WJ (1969) The pigeon retina: quantitative aspects of optic nerve and ganglion cell layer. J Comp Neurol 137:1–18

Bock WJ (1994) Concepts and methods in ecomorphology. J Biosci 19:403–413

Boire D, Dufour JS, Theoret H, Ptito M (2001) Quantitative analysis of the retinal ganglion cell layer in the ostrich, *Struthio camelus*. Brain Behav Evol 58:343–355

Braekevelt CR (1990) Retinal photoreceptor fine structure in the mallard duck (*Anas platyrhynchos*). Histol Histopath 5:123–131

Budnik V, Mpodozis J, Varela FJ, Maturana HR (1984) Regional specialization of the quail retina: ganglion cell density and oil droplet distribution. Neurosci Lett 51:145–150

Chen Y, Naito J (1999) A quantitative analysis of the cells in the ganglion cell layer of the chick retina. Brain Behav Evol 53:75–86

Coimbra JP, Marceliano MLV, Andrade-da-Costa BLS, Yamada ES (2006) The retina of tyrant flycatchers: topographic organization of neuronal density and size in the ganglion cell layer of the great kiskadee *Pitangus sulphuratus* and the rusty marginated flycatcher *Myiozetetes cayanensis* (Aves: Tyrannidae). Brain Behav Evol 68:15–25

Coimbra JP, Trévia N, Marceliano ML, da Silveira Andrade-Da-Costa BL, Picanço-Diniz CW, Yamada ES (2009) Number and distribution of neurons in the retinal ganglion cell layer in relation to foraging behaviors of tyrant flycatchers. J Comp Neurol 514:66–73

Coimbra JP, Nolan PM, Collin SP, Hart NS (2012) Retinal ganglion cell topography and spatial resolving power in penguins. Brain Behav Evol 80:254–268

Collin SP (1999) Behavioural ecology and retinal cell topography. In: Archer SN, Djamgoz MBS, Loew ER, Partridge JC, Vellarga S (eds) Adaptive mechanisms in the ecology of vision. Kluwer, Dordrecht, pp 509–535

Collin SP (2008) A web-based archive for topographic maps of retinal cell distribution in vertebrates. Clin Exp Optom 91:85–95

Collin SP, Ali MA (1994) Multiple areas of acute vision in two freshwater teleosts, the creek chub, *Semotilus atromaculatus* (Mitchell) and the cutlips minnow, *Exoglossum maxillingua* (Lesueur). Can J Zool 72:721–730

Collin SP, Hoskins RV, Partridge JC (1998) Seven retinal specializations in the tubular eye of the deep-sea pearleye, *Scopelarchus michaelsarsi*: a case study in visual optimization. Brain Behav Evol 51:291–314

Corfield JR, Gsell AC, Brunton D, Heesy CP, Hall MI, Acosta ML, Iwaniuk AN (2011) Anatomical specializations for nocturnality in a critically endangered parrot, the kakapo (*Strigops habroptilus*). PLoS ONE 6:e22945

Custer CM, Custer TW, Sparks DW (1996) Radio telemetry documents 24-hour feeding activity of wintering lesser scaup. Wilson Bull 108:556–566

del Hoyo J, Elliott A, Sargatal J (1992) Handbook of the birds of the world. Ostrich to Ducks, vol 1. Lynx Edicions, Barcelona

Dolan T, Fernández-Juricic E (2010) Retinal ganglion cell topography of five species of ground-foraging birds. Brain Behav Evol 75:111–121

Duijm M (1958) On the position of a ribbon like central area in the eyes of some birds. Arch Neerl Zool 13:128–145

Ehrlich D (1981) Regional specialization of the chick retina as revealed by the size and density of neurons in the ganglion cell layer. J Comp Neurol 195:643–657

Ehrlich D, Morgan IG (1980) Kainic acid destroys displaced amacrine cells in post-hatch chicken retina. Neurosci Lett 17:43–48

Fernández-Juricic E, Moore BA, Doppler M, Freeman J, Blackwell BF, Lima SL, DeVault TL (2011) Testing the terrain hypothesis: Canada geese see their world laterally and obliquely. Brain Behav Evol 77:147–158

Fite KV (1973) Anatomical and behavioral correlates of visual acuity in the great horned owl. Vision Res 13:219–230

Fite KV, Rosenfield-Wessels S (1975) A comparative study of deep avian foveas. Brain Behav Evol 12:97–115

Gislén A, Dacke M, Kröger RHH, Abrahamsson M, Nilsson D-E, Warrant EJ (2003) Superior underwater vision in a human population of sea gypsies. Curr Biol 13:833–836

Goodman DC, Fisher H (1962) Functional morphology of the feeding apparatus in waterfowl, Aves: Anatidae. Southern Illinois University Press, Carbondale

Gottschaldt KM, Lausmann S (1974) The peripheral morphological basis of tactile sensibility in the beak of geese. Cell Tissue Res 153:477–496

Guillemain M, Fritz H, Guillon N, Simon G (2002a) Ecomorphology and coexistence in dabbling ducks: the role of lamellar density and body length in winter. Oikos 98:547–551

Guillemain M, Martin GR, Fritz H (2002b) Feeding methods, visual fields and vigilance in dabbling ducks (Anatidae). Funct Ecol 16:522–529

Guillemain M, Fritz H, Duncan P (2002c) The importance of protected areas as nocturnal feeding grounds for dabbling ducks wintering in western France. Biol Conserv 103:183–198

Gundersen HJG (1977) Notes on the estimation of the numerical density of arbitrary particles: the edge effect. J Microsc 111:219–223

Gurd DB (2007) Predicting resource partitioning and community organization of filter-feeding dabbling ducks from functional morphology. Am Nat 169:334–343

Gutiérrez-Ibáñez C, Iwaniuk AN, Wylie DR (2009) The independent evolution of the enlargement of the principal sensory nucleus of the trigeminal nerve in three different groups of birds. Brain Behav Evol 74:280–294

Hall MI, Ross CF (2007) Eye shape and activity pattern in birds. J Zool 271:437–444

Hart NS (2001) Variations in cone photoreceptor abundance and the visual ecology of birds. J Comp Physiol A 187:685–697

Hart NS (2002) Vision in the peafowl (Aves: *Pavo cristatus*). J Exp Biol 205:3925–3935

Hayes BP (1984) Cell populations of the ganglion cell layer: displaced amacrine and matching amacrine cells in the pigeon retina. Exp Brain Res 56:565–573

Hayes BP, Brooke MD (1990) Retinal ganglion cell distribution and behavior in Procellariiform seabirds. Vision Res 30:1277–1289

Hayes BP, Holden AL (1983) The distribution of displaced ganglion cells in the retina of the pigeon. Exp Brain Res 49:181–188

Hayes BP, Hodos W, Holden AL, Low JC (1987) The projection of the visual field upon the retina of the pigeon. Vision Res 27:31–40

Hayes BP, Martin GR, Brooke M de L (1991) Novel area subserving binocular vision in the retinae of Procellariiform seabirds. Brain Behav Evol 37:79–84

Heppner FH, Convissar JL, Moonan DE Jr, Anderson JGT (1965) Visual angle and formation flight in Canada geese (*Branta canadensis*). Auk 102:195–198

Hughes A (1977) The topography of vision in mammals of contrasting lifestyles: comparative optics and retinal organization. In: Cresitelli F (ed) Handbook of sensory physiology vol VIII/5. Springer, Berlin, pp 613–756

Hughes A (1985) New perspectives in retinal organization. In: Osbourne NN, Chader G (eds) Progress in retinal research. Pergamon Press, New York, pp 243–313

Ikushima M, Watanabe M, Ito H (1986) Distribution and morphology of retinal ganglion cells in the Japanese quail. Brain Res 376:320–334

Inzunza O, Bravo H, Smith RL, Angel M (1991) Topography and morphology of retinal ganglion cells in Falconiforms: a study on predatory and carrion-eating birds. Anat Rec 229:271–277

Iwaniuk AN, Heesy CP, Hall MI (2010a) Morphometrics of the eyes and orbits of the nocturnal swallow-tailed gull (*Creagrus furcatus*). Can J Zool 88:855–865

Iwaniuk AN, Gutiérrez-Ibáñez C, Pakan JMP, Wylie DR (2010b) Allometric scaling of the tectofugal pathway in birds. Brain Behav Evol 75:122–137

Jane SD, Bowmaker JK (1988) Tetrachromatic colour vision in the duck (*Anas platyrhynchos* L.): microspectrophotometry of visual pigments and oil droplets. J Comp Physiol A 162:225–235

Johnsgard PA (1965) Handbook of waterfowl behavior. Cornell University Press, Ithaca

Johnsgard PA (1978) Ducks, geese, and swans of the world. University of Nebraska Press, Lincoln

Jorde DG, Owen RB (1988) The need for nocturnal activity and energy budgets of waterfowl. In: Weller MW (ed) Waterfowl in winter. University of Minnesota Press, Minneapolis, pp 169–180

Kear J, Burton PJK (1971) The food and feeding apparatus of the blue duck *Hymenolaimus*. Ibis 113:483–493

Kehoe FP, Thomas VG (1987) A comparison of interspecific differences in the morphology of the external and internal feeding apparatus among North American Anatidae. Can J Zool 65:1818–1822

Kirk EC (2004) Comparative morphology of the eye in primates. Anat Rec 281A:1095–1103

Kirk EC (2006) Eye morphology in cathemeral lemurids and other mammals. Folia Primatol 77:27–49

Krogis A (1931) On the topography of the Herbst's and Grandry's corpuscles in the adult and embryonic duck-bill. Acta Zool (Stockh) 12:241–263

Land MF (1999) The roles of head movements in the search and capture strategy of a tern (Aves, Laridae). J Comp Physiol A 184:265–272

Land MF, Nilsson D-E (2002) Animal eyes. Oxford University Press, Oxford

Leitner L-M, Roumy M (1974) Mechanosensitive units in the upper bill and in the tongue of the domestic duck. Pflügers Arch 346:141–150

Lessells CM, Boag PT (1987) Unrepeatable repeatabilities: a common mistake. Auk 104:116–121

Levy B, Sivak JG (1980) Mechanisms of accommodation in the bird eye. J Comp Physiol 137:267–272

Lewis TL, Esler D, Boyd WS, Zydelis R (2005) Nocturnal foraging behavior of wintering surf scoters and white-winged scoters. Condor 107:637–647

Lisney TJ, Collin SP (2008) Retinal ganglion cell distribution and spatial resolving power in elasmobranchs. Brain Behav Evol 72:59–77

Lisney TJ, Iwaniuk AN, Bandet MV, Wylie DW (2012a) Eye shape and retinal topography in owls (Aves: Strigiformes). Brain Behav Evol 79:218–236

Lisney TJ, Iwaniuk AN, Kolominsky J, Bandet MV, Corfield JR, Wylie DW (2012b) Interspecifc variation in eye shape and retinal topography in seven species of galliform bird (Aves: Galliformes: Phasianidae). J Comp Physiol A 198:717–731

Ma Y, Chen Y, Wang Z, Yang X, Jing H, Lin J (2004) Distribution of displaced amacrine cells in the ganglion cell layer of the Beijing duck retina. J China Agric Univ 9:52–56 [In Chinese with English abstract]

Marshall J, Mellerio J, Palmer DA (1973) A schematic eye for the pigeon. Vision Res 13:2449–2453

Martin GR (1986) Total panoramic vision in the mallard duck *Anas platyrhynchos*. Vision Res 26: 1303–1305

Martin GR (1994a) Form and function in the optical structure of bird eyes. In: Davies MNO, Green PR (eds) Perception and motor control in birds. Springer, Berlin, pp 5–34

Martin GR (1994b) Visual fields in woodcocks *Scolopax rusticola* (Scolopacidae; Charadriiformes). J Comp Physiol A 174:787–793

Martin GR, Katzir G (1999) Visual fields in short-toed eagles, *Circaetus gallicus* (Accipitridae), and the function of binocularity in birds. Brain Behav Evol 53:55–66

Martin GR, Shaw JM (2010) Bird collisions with power lines: failing to see the way ahead? Biol Conserv 143:2695–2702

Martin GR, Jarrett N, Williams M (2007) Visual fields in blue ducks *Hymenolaimus malacorhynchis* and pink-eared ducks *Malacorhynchus membranaceus*: visual and tactile foraging. Ibis 149:112–120

Mass AM, Supin AY (1995) Ganglion cell topography of the retina in the bottlenosed dolphin, *Tursiops truncates*. Brain Behav Evol 45:257–265

Mass AM, Ketten DR, Odell DK, Supin AY (2011) Ganglion cell distribution and retinal resolution in the Florida manatee, *Trichechus manatus latirostris*. Anat Rec 295:177–186

McNeil R, Drapeau P, Goss-Custard JD (1992) The occurrence and adaptive significance of nocturnal habits in waterfowl. Biol Rev 67:381–419

Meyer DB (1977) The avian eye and its adaptations. In: Cresitelli F (ed) Handbook of sensory physiology, vol VIII/5. Springer, Berlin, pp 549–611

Moore BA, Baumhardt P, Doppler M, Randolet J, Blackwell BF, DeVault TL, Loew ER, Fernández-Juricic E (2012) Oblique color vision in an open-habitat bird: spectral sensitivity, photoreceptor distribution and behavioral implications. J Exp Biol 215:3442–3452

Moroney MK, Pettigrew JD (1987) Some observations on the visual optics of kingfishers (Aves, Coraciformes, Alcedinidae). J Comp Physiol A 160:137–149

Nudds TD, Sjöberg K, Lundberg P (1994) Ecomorphological relationships among Palearctic dabbling ducks on Baltic coastal wetlands and a comparison with the Nearctic. Oikos 69: 295–303

Pang JJ, Wu SM (2011) Morphology and immunoreactivity of retrogradely double-labeled ganglion cells in the mouse retina. Invest Ophthalmol Vis Sci 52:4886–4896

Partridge JC (1989) The visual ecology of avian cone oil droplets. J Comp Physiol A 165:415–426

Pettigrew JD, Dreher B, Hopkins CS, McCall MJ, Brown M (1988) Peak density and distribution of ganglion cells in the retinae of microchiropteran bats: implications for visual acuity. Brain Behav Evol 32:39–56

Rahman ML, Sugita S, Aoyama M, Sugita S (2006) Number, distribution and size of retinal ganglion cells in the jungle crow (*Corvus macrorhynchos*). Anat Sci Int 81:253–259

Rahman ML, Aoyama M, Sugita S (2007a) Topography of ganglion cells in the retina of the duck (*Anas platyrhynchis var. domesticus*). Anim Sci J 78:286–292

Rahman ML, Aoyama M, Sugita S (2007b) Regional specialization of the tree sparrow *Passer montanus* retina: ganglion cell density and oil droplet distribution. Ornithol Sci 6:95–105

Rahman ML, Aoyama M, Sugita S (2008) Ganglion cell density and oil droplet distribution in the retina of brown-eared bulbul (*Hysipetes amaurotis*). Anat Sci Int 83:239–246

Rasband WS (1997–2012) Image J. US National Institutes of Health, Bethesda, MD, USA. http://imagej.nih.gov/ij/

Raveling DG (1969) Preflight and flight behavior of Canada geese. Auk 86:671–681

Raveling DG, Crews WE, Klimstra WD (1972) Activity patterns of Canada geese during winter. Wilson Bull 84:278–295

Reymond L (1985) Spatial visual acuity of the eagle *Aquila audax*: a behavioural, optical and anatomical investigation. Vision Res 25:1477–1491

Reymond L (1987) Spatial visual acuity of the falcon, *Falco berigora*: a behavioural, optical and anatomical investigation. Vision Res 27:1859–1874

Rice AN, Westneat MW (2005) Coordination of feeding, locomotor and visual systems in parrotfishes (Teleostei: Labridae). J Exp Biol 208:3503–3518

Rylander MK, Bolen EG (1974) Feeding adaptations in whistling ducks (*Dendrocygna*). Auk 91:86–94

Sargeant AB, Raveling DG (1992) Mortality during the breeding season. In: Batt BDJ, Afton AD, Anderson MG, Ankney CD, Johnson DH, Kadlec JA, Krapu GL (eds) Ecology and management of breeding waterfowl. University of Minnesota Press, Minneapolis, pp 396–422

Scheaffer RL, Mendenhall W, Ott L (1996) Elementary survey sampling, 5th edn. PWS-Kent, Boston

Schiviz AN, Ruf T, Kuebber-Heiss A, Schubert C, Ahnelt PK (2008) Retinal cone topography of artiodactyl mammals: influence of body height and habitat. J Comp Neurol 507:1336–1350

Schmitz C, Hof PR (2000) Recommendations for straightforward and rigorous methods of counting neurons based on a computer simulation approach. J Chem Neuroant 20:93–114

Schmitz L, Wainwright PC (2011) Nocturnality constrains morphological and functional diversity in the eyes of reef fishes. BMC Evol Biol 11:338

Sivak JG, Hildebrand T, Lebert C (1985) Magnitude and rate of accommodation in diving and nondiving birds. Vision Res 25:925–933

Sjöberg K (1985) Foraging activity patterns in the goosander (*Mergus merganser*) and the red-breasted merganser (*M. serrator*) in relation to patterns of activity in their major prey species. Oecologia 67:35–39

Sjöberg K (1988) Food selection, food-seeking patterns and hunting success of captive goosanders *Mergus merganser* and red-breasted mergansers *M. serrator* in relation to the behaviour of their prey. Ibis 130:79–93

Slonaker JR (1897) A comparative study of the area of acute vision in vertebrates. J Morph 13:445–502

Stone J (1981) The wholemount handbook: a guide to the preparation and analysis of retinal wholemounts. Clarendon Press, Sydney

Suburo AM, Herrero MV, Scolaro JA (1991) Regionalization of the ganglion cell layer in the retina of the Magellanic penguin (*Spheniscus magellanicus*). Colonial Waterbirds 14:17–24

Temple SE, Hart NS, Marshall J, Collin SP (2010) A spitting image: specializations in archerfish eyes for vision at the interface between air and water. Proc R Soc Lond B 277:2607–2615

Tome MW, Wrubleski DA (1988) Underwater foraging behavior of canvasbacks, lesser scaups, and ruddy ducks. Condor 90:168–172

Ullmann JFP, Moore BA, Temple SH, Fernández-Juricic E, Collin SP (2012) The retinal wholemount technique: a window to understanding the brain and behaviour. Brain Behav Evol 79:26–44

van der Leeuw AHJ, Kurk K, Snelderwaard PC, Bout RG, Berkhoudt H (2003) Conflicting demands on the tropic system of Anseriformes and their evolutionary implications. Anim Biol 53:259–301

Veilleux CC, Lewis RJ (2011) Effects of habitat light intensity on mammalian eye shape. Anat Rec 294:905–914

Walls GL (1942) The vertebrate eye and its adaptive radiation. Cranbrook Institute of Science, Bloomfield Hills

Wathey JC, Pettigrew JD (1989) Quantitative analysis of the retinal ganglion cell layer and optic nerve of the barn owl *Tyto alba*. Brain Behav Evol 33:279–292

Wood CA (1917) The fundus oculi of birds, especially as viewed by the ophthalmoscope: a study in comparative anatomy and physiology. Lakeside Press, Chicago